The yeast mutant *vps5Δ* affected in the recycling of Golgi membrane proteins displays an enhanced vacuolar Mg^{2+}/H^{+} exchange activity

Gilles Borrelly*†, Jean-Christophe Boyer*‡, Brigitte Touraine, Wojciech Szponarski, Michèle Rambier, and Rémy Gibrat

Biochimie et Physiologie Moléculaire des Plantes§, Ecole Nationale Supérieure d'Agronomie de Montpellier (Agro-M)/Institut National de la Recherche Agronomique, 2 place Viala, 34060 Montpellier cedex 1, France

Edited by Randy Schekman, University of California, Berkeley, CA, and approved May 31, 2001 (received for review May 12, 2000)

Growth of the yeast vacuolar protein-sorting mutant *vps5Δ* affected in the endosome-to-Golgi retromer complex was more sensitive to Mg^{2+}-limiting conditions than was the growth of the wild-type (WT) strain. This sensitivity was enhanced at acidic pH. The *vps5Δ* strain was also sensitive to Al^{3+}, known to inhibit Mg^{2+} uptake in yeast cells. In contrast, it was found to be resistant to Ni^{2+} and Co^{2+}, two cytotoxic analogs of Mg^{2+}. Resistance to Ni^{2+} did not seem to result from the alteration of plasma-membrane transport properties because mutant and WT cells displayed similar Ni^{2+} uptake. After plasma-membrane permeabilization, intracellular Ni^{2+} uptake in *vps5Δ* cells was 3-fold higher than in WT cells, which is consistent with the implication of the vacuole in the observed phenotypes. In reconstituted vacuolar vesicles prepared from *vps5Δ*, the rates of H^{+} exchange with Ni^{2+}, Co^{2+}, and Mg^{2+} were increased (relative to WT) by 170%, 130%, and 50%, respectively. The rates of H^{+} exchange with Ca^{2+}, Cd^{2+}, and K^{+} were similar in both strains, as were α-mannosidase and H^{+}-ATPase activities, and SDS/PAGE patterns of vacuolar proteins. Among 14 other vacuolar protein-sorting mutants tested, only the 8 mutants affected in the recycling of trans-Golgi network membrane proteins shared the same Ni^{2+} resistance phenotype as *vps5Δ*. It is proposed that a trans-Golgi network Mg^{2+}/H^{+} exchanger, mislocalized to *vps5Δ* vacuole, could be responsible for the phenotypes observed *in vivo* and *in vitro*.

Protein sorting pathways from the trans-Golgi network (TGN) to the vacuole have been extensively studied through a large number of yeast mutants (reviewed in refs. 1 and 2). To date, two main intracellular routes have been identified, exemplified by the respective targeting pathways of carboxypeptidase Y (CPY) and alkaline phosphatase (ALP). CPY travels through a prevacuolar/endosomal compartment (PVC) and subsequently onto the vacuole, whereas ALP bypasses the PVC to reach the same organelle. Numerous dedicated proteins localized in transport vesicles or target membranes take part in this process, and the recycling of some of these proteins is important for the efficiency of some trafficking steps. In particular, a membrane-coat complex, designated as the retromer complex, is essential for the PVC-to-Golgi retrograde vesicular transport (3). The retromer complex assembles from two subcomplexes composed of Vps35p/Vps29p/Vps26p and Vps5p/Vps17p, respectively. The first subcomplex is thought to select cargo for retrieval, whereas the second would promote vesicle formation (3–5). Mutation of *VPS5*, a nonessential gene, causes the secretion of CPY (6, 7). Indeed, Vps5p is required for the PVC-to-Golgi retrieval of Vps10p, a membrane protein that ensures binding and Golgi-to-PVC transport of CPY. Consequently, Vps10p is misrouted to the vacuole membrane in *vps5* mutants, whereas CPY accumulates in the Golgi and is then secreted.

In this study, a *vps5Δ* strain is shown to display new growth phenotypes toward Mg^{2+}-limiting media or media containing the Mg^{2+} cytotoxic analogs Ni^{2+} and Co^{2+}. Together with *in vivo* assays of Ni^{2+} uptake and *in vitro* assays of vacuolar C^{2+} (divalent cation)/H^{+} exchange, our data suggest that the phenotypes originate from an enhanced vacuolar compartmentalization of C^{2+} mediated by a Mg^{2+}/H^{+} exchange mechanism.

Materials and Methods

Strains, Media, and Spot Assays. The haploid *Saccharomyces cerevisiae* wild-type (WT) strain Hansen BY4741 (ref. 8; genotype: *MAT***a** *his3-1 leu2-0 met15-0 ura3-0*) was obtained from the American Type Culture Collection, and the *vps* mutants were obtained from Research Genetics (Huntsville, AL). Yeast strains were propagated in standard yeast nitrogen base (YNB) minimal medium (9). To screen heavy metal resistance phenotypes, medium was prepared from a YNB powder containing ammonium sulfate but no C^{2+} (Bio 101). The YNB powder was complemented with glucose and Ca^{2+}, Cu^{2+}, Fe^{2+}, Mg^{2+}, Mn^{2+}, and Zn^{2+} up to standard concentrations (9), except for Mg^{2+}, which was adjusted to 100 μM. A supplemental mixture (CSM, Bio 101) was added according to manufacturer's instructions, and agar was used as the gelling agent (14 g·liter^{-1}). After autoclaving, heavy metals to which resistance was tested were added in the medium at the desired concentrations. Sensitivity to Mg^{2+}-limiting conditions was studied on a similar YNB minimal medium, except that agar was replaced by a low-Mg^{2+}-containing agarose (12 g·liter^{-1}; Low EEO, Sigma). This medium did not allow yeast growth without Mg^{2+} supplementation (data not shown). Magnesium was added at the indicated concentrations after autoclaving. The pH of YNB minimal media was 4.3. When required, the pH was adjusted before autoclaving with HCl to pH 3.0, with 50 mM succinate/KOH to pH 4.3 or 5.6, or with 50 mM Hepes/KOH to pH 7.5.

Spot assays were performed with strains grown up to stationary phase in standard YNB minimal medium (OD_{600} = 6). Ten microliters of diluted cultures (OD_{600} = 0.02) was laid on plates containing the selective media, and growth phenotypes were documented daily with a video imaging system. A wide range of ion conditions was tested; only representative conditions were chosen for the figures presented below. For Ni^{2+} uptake or tonoplast isolation, strains were grown to mid-logarithmic phase

This paper was submitted directly (Track II) to the PNAS office.

Abbreviations: TGN, trans-Golgi network; CPY, carboxypeptidase Y; PVC, prevacuolar compartment; C^{2+}, divalent cation; WT, wild type; ACMA, 9-amino-6-chloro-2-methoxyacridine; ^{R} and ^{S}, resistant and sensitive.

*G.B. and J.-C.B. contributed equally to this work.

†Present address: Biochemistry and Genetics, Medical School, University of Newcastle, Newcastle-Upon-Tyne NE2 4HH, United Kingdom.

‡To whom reprint requests should be addressed at: Biochimie & Physiologie Moléculaire des Plantes, Unité Mixte de Recherche 5004 (Agro de Montpellier, Centre National de la Recherche Scientifique, Institut National de la Recherche Agronomique, Université Montpellier II), ENSA-M/INRA, 34060 Montpellier cedex 1, France. E-mail: boyer@ensam.inra.fr.

§Unité Mixte de Recherche 5004 (Agro de Montpellier, Centre National de la Recherche Scientifique, Institut National de la Recherche Agronomique, Université Montpellier II).

The publication costs of this article were defrayed in part by page charge payment. This article must therefore be hereby marked "*advertisement*" in accordance with 18 U.S.C. §1734 solely to indicate this fact.

www.pnas.org/cgi/doi/10.1073/pnas.161215198

($OD_{600} \approx 3$) in standard YNB minimal medium. Cells were harvested by centrifugation at 4,400 × *g* for 5 min. Pellets were washed at room temperature in water and resuspended in the buffers indicated below.

Vacuole Isolation, Biochemical Assays. According to Roberts *et al.* (10), yeast cells were resuspended in Zymolyase-containing buffer to be converted to spheroplasts, and after osmotic lysis in the presence of a yeast protease inhibitor mixture (Sigma), vacuoles were purified by flotation on a discontinuous Ficoll gradient. After elimination of lipid particles (11), vacuoles were fragmented, and tonoplast vesicles were pelleted and resuspended in 2 mM Tris·HCl, pH 7.5/250 mM sorbitol/2 mM DTT/20% (vol/vol) glycerol and stored in liquid nitrogen. V-ATPase and α-mannosidase activities were measured as described by Lichko *et al.* (12) and Roberts *et al.* (10). SDS/PAGE of tonoplast proteins was performed according to Laemmli (13). Gels were silver-stained (14) and analyzed with IMAGEMASTER image analysis software (Amersham Pharmacia). Cell fractionation experiments using differential centrifugation to separate P150 and P13 membrane fractions from the cytosolic fraction (S150) were performed essentially as described (15). First, the purity of vacuolar membrane preparations was assessed from the ATPase activities of plasma membrane and mitochondria, according to Landolt-Marticorena *et al.* (16). Second, Western blotting was performed by using monoclonal antibodies (Molecular Probes) against Vph1p (dilution 1:2,000), Pep12p (1:600), Dpm1p (1:400), CoxIIIp (1:1,000), and Vps10p (1:400). Proteins were immunodetected by using a chemiluminescent assay (Aurora, ICN). Protein concentrations were determined by the Schaffner and Weissman method (17), using BSA as a standard.

C^{2+}/H^+ Exchange *in Vitro*. Tonoplast proteins were inserted into soybean liposomes essentially as described (18), except for the following. The detergent octyl glucoside was eliminated by using Sephadex G-50 minicolumns (Amersham Pharmacia) (19). Reconstitution was performed at a lipid/protein ratio of 30 (wt/wt). The reconstitution buffer contained 5 mM EDTA (Na^+-free), adjusted to pH 5.5 with 1,3-bis[tris(hydroxymethyl)-methylamino]propane and then adjusted to pH 7.0 with NH_4OH, 0.4 M sorbitol, and glycerol to a final concentration of 20% (vol/vol). Reconstituted tonoplast vesicles were diluted 200-fold in a stirred cuvette (1 ml) containing a NH_4^+-free assay buffer (5 mM LiHepes, pH 7.5/0.4 M sorbitol) and the fluorescent permeant pH probe 9-amino-6-chloro-2-methoxyacridine (ACMA) at 1 μM. The NH_4^+ dilution resulted in an acid-loading of the vesicles, caused by the outward diffusion of NH_3 (20). Transmembrane ΔpH was monitored by the fluorescence quenching of ACMA measured at 415/485 nm. Thereafter, quasi-infinite inward gradients of the indicated C^{2+} were imposed by adding C^{2+} to the outside. C^{2+}/H^+ exchangers used this gradient to generate divalent influxes coupled to H^+ efflux, estimated by the initial rate of dissipation of the ACMA quenching (determined from the derivation of the kinetics). This initial rate, named V_{H^+}, was linear with the protein concentration (data not shown) and is expressed in %·min^{-1} per mg of protein.

$^{63}Ni^{2+}$ Uptake. The yeast pellet was resuspended (final OD_{600} = 4) in 5 mM Tris·succinate, pH 4.3/2% (wt/vol) glucose/50 mM KCl. This suspension (900 μl) was incubated for 30 min at 30°C under constant agitation (80 rpm). Nickel uptake was initiated by the addition of ^{63}Ni (6.14 MBq·$mmol^{-1}$ $^{63}NiCl_2$, DuPont) at 3.5 μM final concentration and 250 μM $NiCl_2$. The uptake was stopped at different times by the filtration of 100-μl aliquots on 0.45-μm pore nitrocellulose membranes (Millipore). Filters were washed three times with 10 ml of 40 mM $NiCl_2$; radioactivity retained on filters was measured by using a liquid scintillation analyzer. $^{63}Ni^{2+}$ contents were expressed in mmol per mg^{-1} dry weight. $^{63}Ni^{2+}$ uptake experiments on permeabilized yeast cells were performed at pH 6.9 as described (21, 22) and in the same conditions as above.

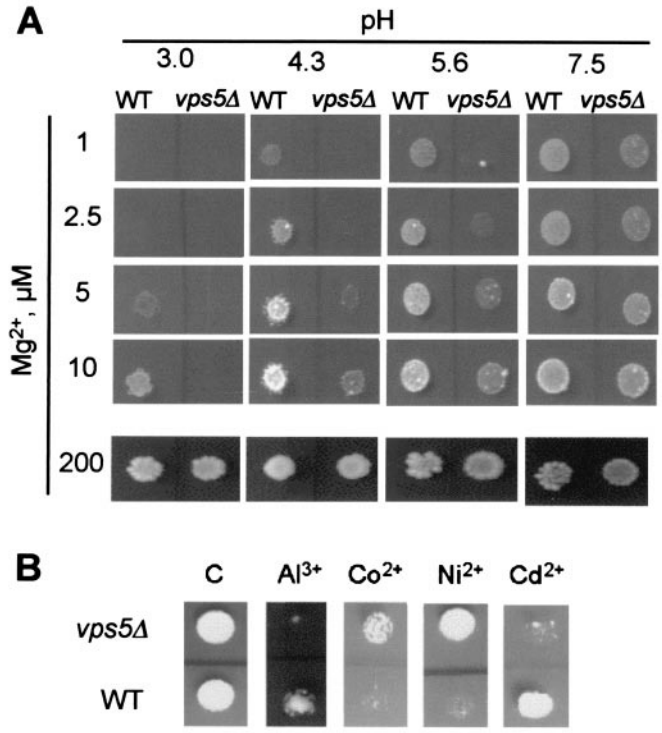

Fig. 1. Growth phenotypes of *vps5*Δ and WT. (*A*) pH-dependent phenotypes in Mg^{2+}-limiting media. Spot assays were recorded after 5-days (200 μM Mg^{2+}, Mg^{2+}-nonlimiting condition) or 10-days of growth (other assays, Mg^{2+}-limiting conditions) on an agarose/YNB minimal medium at the indicated pH and Mg^{2+} concentrations. (*B*) Tolerance to cytotoxic heavy metals. Spot assays were recorded after 6-days of growth on an agar/YNB minimal medium (pH 4.3) containing 0.1 mM Mg^{2+} (nonlimiting), and the following concentrations of the indicated metals: 1 mM Al^{3+}, 0.5 mM Co^{2+}, 0.25 mM Ni^{2+}, and 0.25 mM Cd^{2+}. C, control plate.

Results

On Mg^{2+} nonlimiting solid media, the *vps5*Δ and WT strains displayed a similar growth capacity at any pH tested (pH 3.0 to 7.5; Fig. 1*A*). In contrast, on Mg^{2+}-limiting media, the growth capacity of both strains was impaired upon medium acidification. Importantly, *vps5*Δ exhibited a stronger sensitivity than WT to such acidification in low-Mg^{2+} conditions. This phenotype is called low-Mg^S in the rest of this paper.

The *vps5*Δ strain also showed contrasting phenotypes in response to heavy metals in nonlimiting Mg^{2+} conditions (Fig. 1*B*). Relative to WT, the *vps5*Δ strain was resistant to Ni^{2+} and to Co^{2+} (Ni^R and Co^R phenotypes) but sensitive to Al^{3+} and Cd^{2+} (Al^S and Cd^S phenotypes). The kinetics of $^{63}Ni^{2+}$ uptake by *vps5*Δ and WT cells were similar (Fig. 2*A*). However, after plasma-membrane permeabilization (21, 22), the intracellular $^{63}Ni^{2+}$ uptake by *vps5*Δ cells reached a level 3-fold higher after 6 hr (Fig. 2*B*). Tonoplast vesicles were prepared from Ficoll gradient-purified vacuoles as indicated in *Materials and Methods*. The isolation yields of tonoplast proteins per g fresh weight of the two strains were similar, as well as the activities of the tonoplast enzyme markers V-ATPase and α-mannosidase (Fig. 3*A*). Inhibition of the total ATP hydrolysis activity by bafilomycin was about 70%, whereas inhibition by oligomycin and vanadate was less than 10%, indicating minimal contamination

CELL BIOLOGY

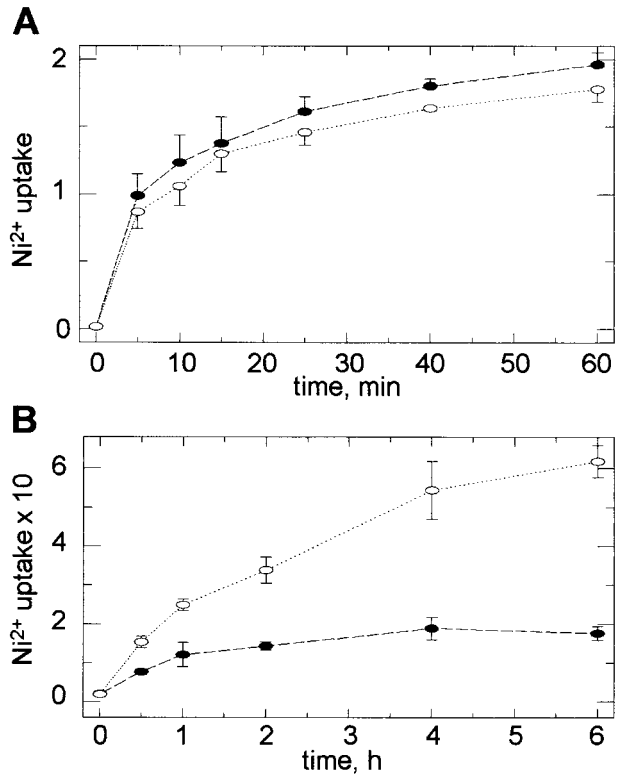

Fig. 2. $^{63}Ni^{2+}$ uptake by *vps5*Δ and WT cells. (*A*) Control cells. (*B*) Cells with permeabilized plasma membrane. Values for WT (●) and *vps5*Δ (○) are presented as mean ± SE ($n = 3$). The uptake is expressed as mmol of Ni^{2+} per mg of dry weight.

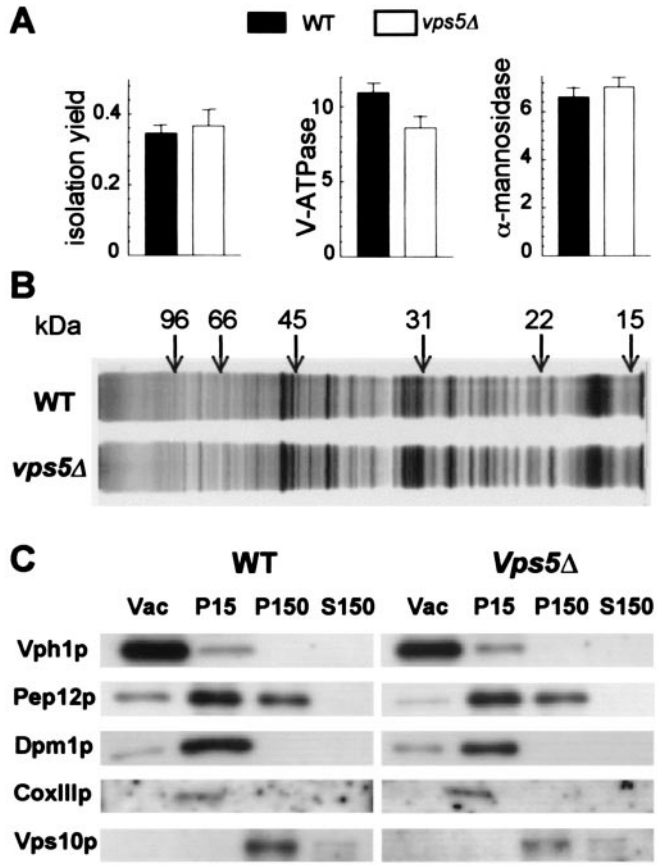

Fig. 3. Biochemical properties of tonoplast isolated from *vps5*Δ and WT. (*A*) Isolation yield, hydrolytic activity of V-ATPase and α-mannosidase expressed in mg of protein per g of fresh weight, μmol of ATP hydrolyzed per hr per mg of protein, and nmol of nitrophenol per min per mg of protein, respectively. These activities were not significantly different between the two strains (Student's *t* tests, data not shown). (*B*) In SDS/PAGE patterns of tonoplast proteins, 62 bands were detected in both patterns with image analysis software. (*C*) Western blot analysis of vacuole membrane (Vac) and subcellular P15, P150, and S150 fractions from WT and *vps5*Δ strains. For a given antibody, equal amounts of fraction proteins were loaded. Monoclonal antibodies were directed against membrane markers of the tonoplast (Vph1p), PVC (Pep12p), endoplasmic reticulum (Dpm1p), mitochondria (CoxIIIp), and TGN (Vps10p).

by mitochondrial and plasma membranes, respectively. SDS/PAGE patterns of tonoplast proteins were indistinguishable (Fig. 3*B*). Fig. 3C shows Western blot analyses performed on vacuolar membrane preparations and subcellular P15, P150, and S150 fractions from WT and mutant by using monoclonal antibodies directed against membrane markers of the tonoplast (Vph1p), mitochondria (CoxIIIp), endoplasmic reticulum (Dpm1p), PVC (Pep12p), and TGN (Vps10p). These data indicate that the vacuolar preparations are highly enriched in vacuolar membrane proteins, which is in agreement with previous studies (11). Contaminations with endoplasmic reticulum and PVC were minor and comparable for both strains, whereas contaminations with mitochondria and TGN were not detectable.

Initial trials (not shown) showed that the filling kinetics of native tonoplast vesicles with C^{2+} in exchange with H^+ were too fast to determine the initial rate of the exchange (V_{H^+}). Therefore, the latter was assayed on reconstituted vesicles to slow down the transport reaction (23). We showed that a similar reconstitution of a plant tonoplast Mg^{2+}/H^+ exchanger allowed for the recovery of the same affinity for Mg^{2+} and sensitivity to inhibitors as at the native membrane level (18). V_{H^+} was measured after an initial acid-loading step was performed as described in *Materials and Methods*. The initial fluorescence quenching of the pH probe ACMA could be totally dissipated by NH_4^+ addition. This result ascertained the instantaneous establishment of a stable transmembrane ΔpH upon acid-loading (Fig. 4). In control liposomes, the addition of Ni^{2+} (or other cations used in this study) to the outside caused a negligible dissipation of ΔpH, as compared with that observed with reconstituted tonoplast vesicles (Fig. 4). Relative to WT, a 2.7-fold higher initial rate of Ni^{2+}/H^+ exchange was observed with reconstituted vesicles from *vps5*Δ.

Selectivity of C^{2+}/proton exchange of reconstituted tonoplast vesicles from *vps5*Δ and WT was compared (Fig. 5). In *vps5*Δ vesicles, V_{H^+} for Mg^{2+}, Co^{2+}, or Ni^{2+} increased by 50%, 130%, and 170%, respectively, compared with WT. In contrast, V_{H^+} with Ca^{2+}, Cd^{2+}, or K^+ was similar for both strains.

To determine the kinetic parameters of the Mg^{2+}/H^+ exchange, V_{H^+} was measured at various Mg^{2+} concentrations (Fig. 6*A*). Scatchard plots were linear (Fig. 6*B*), indicating that the facilitated exchange reaction could be fitted to the classical Michaelian model. The enhanced V_{H^+} in *vps5*Δ-reconstituted tonoplast vesicles resulted from an increase of the V_{max} parameter relative to that of WT, whereas K_m was found at about 1 M for both strains.

Finally, Ni^{2+} growth phenotypes of 14 other yeast mutants of the vacuolar protein sorting pathway were determined (Fig. 7). Eight of these mutants also were shown to be defective in the retention of TGN membrane proteins: two other retromer complex mutants *vps17*Δ and *vps29*Δ (3), *vps54*Δ (24), *vps1*Δ (25), *vps8*Δ (26), *tlg2*Δ (27), *vps13/soi1*Δ (15), and *grd19*Δ (28). All these mutants displayed a Ni^R phenotype. In contrast, six

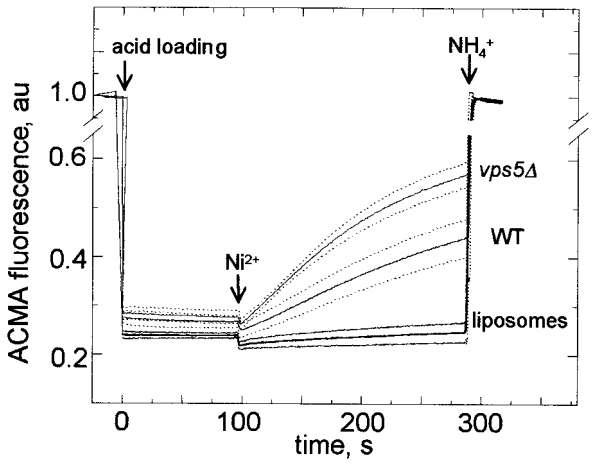

Fig. 4. Activity of Ni^{2+}/H^+ exchange in reconstituted tonoplast vesicles from *vps5*Δ and WT. Ammonium-containing vesicles were diluted 200-fold in the assay buffer free of NH_4^+, causing vesicle acid-loading and instant quenching of the permeant pH probe ACMA. Fluorescence recovery after the addition of 0.5 mM Ni^{2+} to reconstituted tonoplast vesicles, not observed on control liposomes, ascertained the facilitated exchange activity. The final addition of NH_4^+ (15 mM) to the outside allowed the total dissipation of the pH gradient. Solid and dotted lines represent the mean ACMA fluorescence in arbitrary units (au) ± SE (n = 5), respectively.

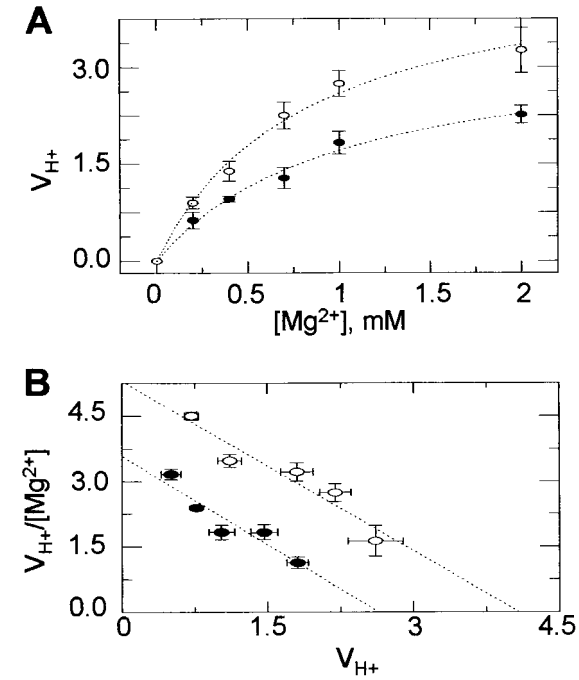

Fig. 6. Mg^{2+}/H^+ exchange rate of reconstituted tonoplast vesicles from *vps5*Δ (○) or WT (●) as a function of Mg^{2+} concentration. (*A*) Exchange rates (V_{H+}) were determined from experimental kinetics illustrated in Fig. 4 and described in *Materials and Methods*. Values are presented as mean V_{H+} ± SE (n = 5). (*B*) Scatchard plot: K_m values derived from linear regression of data in *A* are 0.96 ± 0.02 mM and 0.92 ± 0.01 mM for *vps5*Δ and WT strains, respectively; V_{max} are 4.53 ± 0.36 and 2.93 ± 0.26%·min^{-1} per mg of protein.

other mutants, for which no alteration of this TGN retention process was described, showed a Ni^S phenotype: *vps39*Δ (29), *vps41*Δ (30), *vam3*Δ (31), *vam7*Δ (32), *vps18*Δ (33), and *apl6*Δ (34).

Discussion

The *vps5*Δ Mutant Strain Displays an Enhanced Vacuolar Mg^{2+} (Ni^{2+}, Co^{2+})/H^+Exchange Activity. The *vps5*Δ strain belongs to class B *vps* mutants (35) and displays fragmented vacuoles (refs. 6 and 7; data not shown). However, no gross alteration of functional properties of the *vps5*Δ vacuole could be observed at the cellular level (35, 36). The present study confirms this conclusion at the biochemical level: the isolated vacuole membranes of WT and *vps5*Δ exhibit the same SDS/PAGE protein profiles, α-mannosidase and V-ATPase activities, and H^+ exchange activities with K^+, Ca^{2+}, and Cd^{2+}.

In contrast, we found that the vacuole membrane isolated from *vps5*Δ displays a higher H^+ exchange activity with Mg^{2+}, Ni^{2+}, and Co^{2+}. Ni^{2+} and Co^{2+} are two Mg^{2+} analogs commonly used to trace Mg^{2+} transport (37–42). They are not required for normal yeast growth and are usually omitted from standard growth media. Moreover, significant H^+ exchange activities with these cytotoxic heavy metals were observed only at high con-

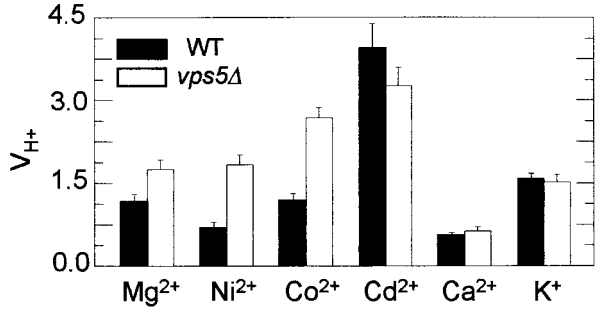

Fig. 5. Selectivity of cation/proton exchange across reconstituted tonoplast vesicles from *vps5*Δ or WT. Cation concentration was 0.5 mM, except for Cd^{2+}, which was 0.2 mM. Exchange rates (V_{H+}) are presented as mean V_{H+} ± SE (n = 3), except for Mg^{2+} (n = 5). Exchange rates were significantly different between *vps5*Δ and WT for Mg^{2+}, Co^{2+}, and Ni^{2+}, but not for Cd^{2+}, Ca^{2+}, and K^+ (Student's t tests, data not shown).

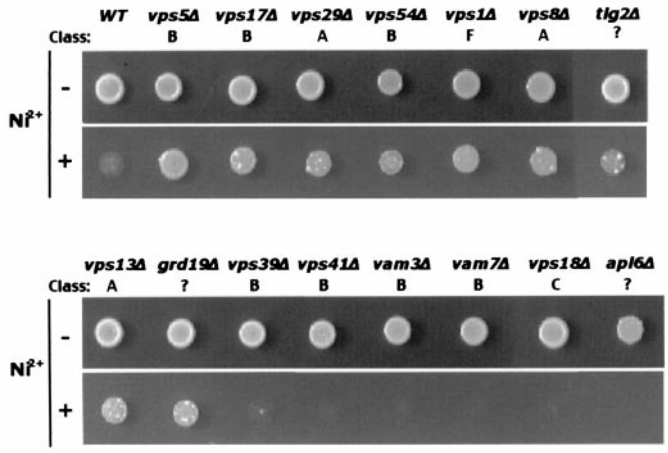

Fig. 7. Ni^{2+} growth phenotypes of yeast mutants of the vacuolar protein-sorting pathway. Mutants were grown on agar/YNB minimal medium containing 0.1 mM Mg^{2+}, with (+) or without (−) 0.2 mM Ni^{2+}. Phenotypes were recorded after 4 days. Class (34) and name of each mutant are indicated. ? indicates class not determined or not available in the literature. Among these mutants, only Ni^{2+}-resistant mutants were found to be defective in the retention of Golgi membrane proteins. We refer the reader to the Yeast Proteome Database (http://www.proteome.com) for further information about the mutants and the corresponding genes (including alternative names and functional details).

CELL BIOLOGY

centrations (0.1 to 1 mM, data not shown), indicating that vacuolar Co^{2+}/H^+ and Ni^{2+}/H^+ exchanges are unlikely to play a physiological role in yeast in standard growth conditions. Conversely, the affinity of the H^+ exchange with Mg^{2+} seems physiologically sound because it displayed a K_m for Mg^{2+} at about 1 mM, close to the reported activity of Mg^{2+} in the yeast cytosol (43). Moreover, the yeast vacuole has been described as an essential Mg^{2+} reservoir (44). The present work provides direct evidence for the activity of a Mg^{2+}/H^+ transport system at the tonoplast of *S. cerevisiae*. The plant vacuolar protein AtMHX was proposed to be an Mg^{2+}/H^+ exchanger (45). Nevertheless, no clear homologue could be detected in yeast.

C^{2+}/H^+ exchangers have been shown to promote a net vacuolar uptake of C^{2+}, driven by the exergonic efflux of H^+ out of acidic vacuoles in yeast cells (46–48). Thus, the rate of vacuolar uptake by C^{2+}/H^+ exchangers is expected to depend on the size of the ΔpH. In the present study, WT and *vps5*Δ exhibited similar vacuolar H^+-ATPase activities. Furthermore, their growth capacity at pH 7.5, known to depend on the presence of a functional vacuolar H^+-ATPase (49, 50), was similar on standard media. In agreement with published data (6, 35), the vacuole should be energized by similar ΔpH in both strains.

In conclusion, the vacuole membrane of the *vps5*Δ strain was found to exhibit similar biochemical and functional features compared with those of the WT strain, except for an enhanced Mg^{2+} (Ni^{2+}, Co^{2+})/H^+ exchange activity. The latter is expected to mediate a higher vacuolar uptake of C^{2+} in mutant yeast cells. Consistently, Ni^{2+} uptake was 3-fold higher in *vps5*Δ cells than in WT cells after plasma-membrane permeabilization. By comparison, Ni^{2+} uptakes by nonpermeabilized mutant cells and WT cells measured in short-term experiments were the same, indicating that both strains would display similar transport properties at the plasma-membrane level.

The *vps5*Δ Mutant Displays New Growth Phenotypes Likely Related to its Enhanced Vacuolar Mg^{2+} (Ni^{2+}, Co^{2+})/H^+Activity. In the present study, a new selectable growth phenotype is presented for mutants altered in the recycling of Golgi membrane proteins: all mutants tested were resistant to Ni^{2+}. In addition, the *vps5*Δ strain was resistant to Co^{2+}, but sensitive to Cd^{2+}, Al^{3+}, and Mg^{2+}-limiting media.

The vacuole has been described as a major site for Cd^{2+} detoxification (51, 52). As mentioned earlier, *vps5*Δ displays a fragmented vacuome composed of a large number of minivacuoles. Unexpectedly, the amounts of tonoplast isolated per g fresh weight of *vps5*Δ and WT were the same, suggesting that vacuomes of both strains might share the same tonoplast surface area despite their different morphologies. With the same areas but smaller vacuoles, a reduction of the vacuome volume might be expected in mutant cells, which would supposedly be detrimental for metal tolerance. Consistently, the Cd^S phenotype of *vps5*Δ was shared by *vps41*Δ (data not shown) and *vps54*Δ (53), two class B mutants showing fragmented vacuoles (30, 35, 53). In addition, *vps18*Δ, a class C mutant lacking any structure resembling a normal vacuole (35), also displays a Cd^S phenotype (54). Thus, a reduction of the vacuome volume might be responsible for the Cd^S phenotype of *vps5*Δ.

Along the same lines, the sensitivity of *vps41*Δ and *vps18*Δ to Ni^{2+} could be related as well to such a reduction of the vacuome volume. Indeed, the vacuole has been described also as a major site for Ni^{2+} detoxification (48, 55, 56). Because class B mutants, showing fragmented vacuoles, displayed either Ni^S (*vps41*Δ, *vps39*Δ, *vam3*Δ, *vam7*Δ) or Ni^R (*vps5*Δ, *vps17*Δ, *vps54*Δ) phenotypes (Fig. 7), the assumed reduction in size of their vacuome cannot account for the phenotype of Ni^R class B mutants. Therefore, we propose that the Ni^R (and Co^R) phenotypes of *vps5*Δ would result from the marked enhancement of its vacuolar Ni^{2+} (Co^{2+})/H^+ exchange activity. This transport activity would improve Ni^{2+} (Co^{2+}) detoxification by increasing their vacuolar compartmentalization in *vps5*Δ (as shown for Ni^{2+}, Fig. 2).

In contrast, vacuolar sequestration of Mg^{2+} by Mg^{2+}/H^+ exchange should be responsible for both WT and *vps5*Δ growth impairments observed at acidic pH in Mg^{2+}-limiting media (Fig. 1*A*). Importantly, acidic conditions alone were not responsible for this effect because the latter was not observed on media containing nonlimiting Mg^{2+} concentrations. On the other hand, the lower the pH in the medium, the lower the pH in the vacuole (57), and thus, the higher the ΔpH energizing vacuolar ion uptake by cation/proton exchangers. In the present study, an increase of the vacuolar Mg^{2+} uptake is expected at acidic pH. In this condition, the increase of the vacuolar uptake would exceed the low cellular Mg^{2+} uptake occurring in low-Mg^{2+} media, thereby impairing cytosolic Mg^{2+} homeostasis. This result would explain the decrease of yeast growth at acidic pH in low-Mg^{2+} (but not in nonlimiting Mg^{2+}) media, depicted horizontally in Fig. 1*A*. At a given pH, i.e., at a constant vacuolar ΔpH, cellular Mg^{2+} uptake would decrease below vacuolar uptake upon Mg^{2+} deprivation. This imbalance would also impair Mg^{2+} cytosolic homeostasis and would explain the yeast growth decrease depicted vertically in Fig. 1*A*.

In this context, the enhanced vacuolar Mg^{2+}/H^+ activity of *vps5*Δ, relative to that of WT, should be responsible for the higher sensitivity of the mutant to the conditions described above. The Al^S phenotype of *vps5*Δ could be interpreted along the same line, because Al^{3+} toxicity was shown to result from the Al^{3+}-inhibition of Mg^{2+} cellular uptake in yeast (42, 58), thereby mimicking Mg^{2+}-limiting conditions. Finally, it should be noted that the low-Mg^S growth phenotype of *vps5*Δ is clearly observable at acidic pH relative to neutral pH, which is consistent with the implication of the vacuole energization in this phenotype.

Missorting of a TGN Mg^{2+}/H^+ Exchanger to the Vacuole Membrane of *vps5*Δ: A Molecular Hypothesis. One straightforward interpretation of the increase of vacuolar C^{2+}/H^+ exchange activity in *vps5*Δ would be that the endogenous vacuolar exchanger is more active in mutant cells. However, deregulation of this exchanger (resulting, for example, in an increase of the exchanger density at the membrane surface or of the proportion of exchangers in the active state) is expected to increase the V_{max} of the transport reaction without modification of its selectivity. Compared with WT, *vps5*Δ exhibited an increase of the V_{max}, but also a marked alteration of ion selectivity: the selectivity sequence was $Mg^{2+} = Co^{2+} > Ni^{2+}$ for WT and $Co^{2+} > Mg^{2+} = Ni^{2+}$ for *vps5*Δ (Fig. 5). In addition, yeast *vps5* mutants, like *vps17* and *vps29* mutants of the retromer complex and other mutants also altered in the recycling of Golgi membrane proteins (*vps54*Δ, *vps1*Δ, *vps8*Δ, *tlg2*Δ, *vps13*Δ, and *grd19*Δ), have been reported to missort various membrane proteins from the TGN (proteinase Kex2p, Vps10p, or dipeptidyl aminopeptidase A) to the tonoplast (3, 15, 24–28). In our study, all these mutants displayed a Ni^R phenotype, whereas other vacuolar protein sorting mutants not affected in this recycling process displayed a Ni^S phenotype. In this context, it may be hypothesized that *vps5*Δ, and possibly other mutants in retention of Golgi membrane proteins, would also missort a TGN Mg^{2+}/H^+ exchanger to the vacuole membrane of mutant cells. It is noteworthy that the literature data indicate that TGN and endosomal compartments sustain high ΔpH generated by the V-ATPase (59, 60).

In conclusion, our data argue in favor of the coexistence of two kinds of exchangers with distinct selectivities at the vacuolar membrane of *vps5*Δ (and possibly of other Golgi retention-defective mutants). Validation of this working hypothesis will require the molecular identification of yeast Mg^{2+}/H^+ exchang-

ers. In wild-type cells, the TGN Mg^{2+}/H^+ exchanger would be recycled between the PVC and the TGN by the retromer complex and could be involved in the pH regulation of the TGN or Golgi-derived vesicles. Such a regulation is thought to be important for the sorting of secretory cargo and the retrieval of components of the biosynthetic pathway (59, 61). Recently, it has been shown that the VPS44 gene actually encodes the Nhx1p Na^+/H^+ exchanger of the PVC and that it is required for endosomal protein trafficking (62). It is noteworthy that neither Na^+/H^+ nor Ca^{2+}/H^+ exchanges were found to be involved in the regulation of the acidification of TGN vesicles (59).

We thank C. Grignon, P. Doumas, and T. Tranbarger for critical reading of the manuscript. We thank J.-P. Grouzis and J. Rigaud for their expertise in vacuole isolation and biochemical analyses, and M. Enjuto for initial help on yeast culture handling. G.B. was supported by a Fellowship from the Ministère de l'Education Nationale, de la Recherche, et de la Technologie.

1. Bryant, N. J. & Stevens, T. H. (1998) *Microbiol. Mol. Biol. Rev.* **62,** 230–247.
2. Lemmon, S. K. & Traub, L. M. (2000) *Curr. Opin. Cell Biol.* **12,** 457–466.
3. Seaman, M. N., McCaffery, J. M. & Emr, S. D. (1998) *J. Cell Biol.* **142,** 665–681.
4. Nothwehr, S. F., Bruinsma, P. & Strawn, L. A. (1999) *Mol. Biol. Cell* **10,** 875–890.
5. Nothwehr, S. F., Ha, S. A. & Bruinsma, P. (2000) *J. Cell Biol.* **151,** 297–310.
6. Nothwehr, S. F. & Hindes, A. E. (1997) *J. Cell Sci.* **110,** 1063–1072.
7. Horazdovsky, B. F., Davies, B. A., Seaman, M. N., McLaughlin, S. A., Yoon, S. & Emr, S. D. (1997) *Mol. Biol. Cell* **8,** 1529–1541.
8. Brachmann, C. B., Davies, A., Cost, G. J., Caputo, E., Li, J., Hieter, P. & Boeke, J. D. (1998) *Yeast* **14,** 115–132.
9. Sherman, F. (1991) *Methods Enzymol.* **194**, 3–21.
10. Roberts, C. J., Raymond, C. K., Yamashiro, C. T. & Stevens, T. H. (1991) *Methods Enzymol.* **194,** 644–661.
11. Zinser, E. & Daum, G. (1995) *Yeast* **11,** 493–536.
12. Lichko, L. P. & Okorokov, L. A. (1984) *FEBS Lett.* **174,** 233–237.
13. Laemmli, U. K. (1970) *Nature (London)* **227,** 680–685.
14. Oakley, R. B., Kirsch, R. D. & Morris, R. N. (1980) *Anal. Biochem.* **105,** 361–363.
15. Brickner, J. H. & Fuller, R. S. (1997) *J. Cell Biol.* **139,** 23–36.
16. Landolt-Marticorena, C., Williams, K. M., Correa, J., Chen, W. & Manolson, M. F. (2000) *J. Biol. Chem.* **275,** 15449–15457.
17. Schaffner, W. & Weissman, C. (1973) *Anal. Biochem.* **56,** 502–514.
18. Amalou, Z., Gibrat, R., Trouslot, P. & d'Auzac, J. (1994) *Plant Physiol.* **106,** 79–85.
19. Amalou, Z., Enjuto, M., Grouzis, J. P., Prevot, J. C., Jacob, J. L., Grignon, C. & Gibrat, R. (1997) *Plant Physiol. Biochem. (Paris)* **35,** 355–361.
20. Schumaker, K. S. & Sze, H. (1990) *Plant Physiol.* **92,** 340–345.
21. Ohsumi, Y., Kitamoto, K. & Anraku, Y. (1988) *J. Bacteriol.* **170,** 2676–2682.
22. Nass, R., Cunningham, K. W. & Rao, R. (1997) *J. Biol. Chem.* **272,** 26145–26152.
23. Pouliquin, P., Grouzis, J.-P. & Gibrat, R. (1999) *Biophys. J.* **76,** 360–373.
24. Conibear, E. & Stevens, T. H. (2000) *Mol. Biol. Cell* **11,** 305–323.
25. Wilsbach, K. & Payne, G. S. (1993) *EMBO J.* **12,** 3049–3059.
26. Chen, Y. J. & Stevens, T. H. (1996) *Eur. J. Cell Biol.* **70,** 289–297.
27. Holthuis, J. C., Nichols, B. J., Dhruvakumar, S. & Pelham, H. R. (1998) *EMBO J.* **17,** 113–126.
28. Voos, W. & Stevens, T. H. (1998) *J. Cell Biol.* **140,** 577–590.
29. Nakamura, N., Hirata, A., Ohsumi, Y. & Wada, Y. (1997) *J. Biol. Chem.* **272,** 11344–11349.
30. Radisky, D. C., Snyder, W. B., Emr, S. D. & Kaplan, J. (1997) *Proc. Natl. Acad. Sci. USA* **94,** 5662–5666.
31. Darsow, T., Rieder, S. E. & Emr, S. D. (1997) *J. Cell Biol.* **138,** 517–529.
32. Ungermann, C. & Wickner, W. (1998) *EMBO J.* **17,** 3269–3276.
33. Rieder, S. E. & Emr, S. D. (1997) *Mol. Biol. Cell* **8,** 2307–2327.
34. Cowles, C. R., Odorizzi, G., Payne, G. S. & Emr, S. D. (1997) *Cell* **91,** 109–118.
35. Raymond, C. K., Howald-Stevenson, I., Vater, C. A. & Stevens, T. H. (1992) *Mol. Biol. Cell* **3,** 1389–1402.
36. Banta, L. M., Robinson, J. S., Klionsky, D. J. & Emr, S. D. (1988) *J. Cell Biol.* **107,** 1369–1383.
37. Fuhrmann, G. F. & Rothstein, A. (1968) *Biochim. Biophys. Acta* **163,** 325–330.
38. Hmiel, S. P., Snavely, M. D., Miller, C. G. & Maguire, M. E. (1986) *J. Bacteriol.* **168,** 1444–1450.
39. Joho, M., Tarumi, K., Inouhe, M., Tohoyama, H. & Murayama, T. (1991) *Microbios* **67,** 177–186.
40. Snavely, M. D., Gravina, S. A., Cheung, T. T., Miller, C. G. & Maguire, M. E. (1991) *J. Biol. Chem.* **266,** 824–829.
41. Nies, D. H. (1992) *Plasmid* **27,** 17–28.
42. MacDiarmid, C. W. & Gardner, R. C. (1998) *J. Biol. Chem.* **273,** 1727–1732.
43. Zhang, A., Cheng, T. P. O., Wu, X. Y., Altura, B. T. & Altura, B. M. (1997) *Cell. Mol. Life Sci.* **53,** 69–72.
44. Beeler, T., Bruce, K. & Dunn, T. (1997) *Biochem. Biophys. Acta* **1323,** 310–318.
45. Shaul, O., Hilgemann, D. W., de-Almeida-Engler, J., Van Montagu, M., Inze, D. & Galili, G. (1999) *EMBO J.* **18,** 3973–3980.
46. Okorokov, L. A., Kulakovskaya, T. V., Lichko, L. P. & Polorotova, E. V. (1985) *FEBS Lett.* **192,** 303–306.
47. Pozos, T. C., Sekler, I. & Cyert, M. S. (1996) *Mol. Cell. Biol.* **16,** 3730–3741.
48. Nishimura, K., Igarashi, K. & Kakinuma, Y. (1998) *J. Bacteriol.* **180,** 1962–1964.
49. Nelson, H. & Nelson, N. (1990) *Proc. Natl. Acad. Sci. USA* **87,** 3503–3507.
50. Nelson, N. & Harvey, W. R. (1999) *Physiol. Rev.* **79,** 361–385.
51. Ortiz, D. F., Kreppel, L., Speiser, D. M., Scheel, G., McDonald, G. & Ow, D. W. (1992) *EMBO J.* **11,** 3491–3499.
52. Li, Z. S., Lu, Y. P., Zhen, R. G., Szczypka, M., Thiele, D. J. & Rea, P. A. (1997) *Proc. Natl. Acad. Sci. USA* **94,** 42–47.
53. Conboy, M. J. & Cyert, M. S. (2000) *Mol. Biol. Cell* **11,** 2429–2443.
54. Clemens, S., Kim, E. J., Neumann, D. & Schroeder, J. I. (1999) *EMBO J.* **18,** 3325–3333.
55. Joho, M., Ishikawa, Y., Kunikane, M., Inouhe, M., Tohoyama, H. & Murayama, T. (1992) *Microbios* **71,** 149–159.
56. Ramsay, L. M. & Gadd, G. M. (1997) *FEMS Microbiol. Lett.* **152,** 293–298.
57. Carmelo, V., Santos, H. & Sa-Correia, I. (1997) *Biochim. Biophys. Acta* **1325,** 63–70.
58. MacDiarmid, C. W. & Gardner, R. C. (1996) *Plant Physiol.* **112,** 1101–1109.
59. Demaurex, N., Furuya, W., D'Souza, S., Bonifacino, J. S. & Grinstein, S. (1998) *J. Biol. Chem.* **273,** 2044–2051.
60. Nelson, N., Perzov, N., Cohen, A., Hagai, K., Padler, V. & Nelson, H. (2000) *J. Exp. Biol.* **203,** 89–95.
61. Mellman, I. (1992) *J. Exp. Biol.* **172,** 39–45.
62. Bowers, K., Levi, B. P., Patel, F. I. & Stevens, T. H. (2000) *Mol. Biol. Cell* **11,** 4277–4294.